Microporous and Mesoporous Materials 355 (2023) 112571

Contents lists available at ScienceDirect

Microporous and Mesoporous Materials

journal homepage: www.elsevier.com/locate/micromeso

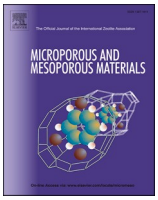

Effect of the presence of mesoporous catalysts in the decomposition of 4-(Methylnitrosoamine)-1-(3-Pyrydyl)-1-Butanone under inert and oxidative atmosphere

J. Asensio [a], M.I. Beltran [a,b], A. Marcilla [a,b,*], D. Berenguer [a]

[a] Inst. Univ. Ingeniería Procesos Químicos, Universidad de Alicante, 03080, Alicante, Spain
[b] Dpto. Ingeniería Química, Universidad de Alicante, 03080, Alicante, Spain

ARTICLE INFO

Keywords:
NNK
Nitrosamine
SBA-15
MCM-41
Pyrolysis
Mesoporous catalysts

ABSTRACT

4-(Methylnitrosoamine)-1-(3-Pyrydyl)-1-Butanone is one of the most toxic substances present in tobacco that comes mainly from the curing process. In this work we have studied the decomposition reactions and the compounds obtained as a function of temperature, under inert atmosphere and air atmosphere. TGA and EGA PY-GC/MS (flash pyrolysis) have been used. The effect of the addition of two SBA-15, with different morphologies (fibres and platelets), and a MCM-41 catalyst were studied. In TGA analysis MCM-41 is the material that produces more changes in the decomposition of this nitrosamine, especially in oxidative atmosphere. The EGA experiments show that 4-(Methylnitrosoamine)-1-(3-Pyrydyl)-1-Butanone is more unstable in air atmosphere and the three materials accelerate the decomposition being MCM-41 followed by SBA-15p those producing the larger modifications in the composition of the gases evolved. All three materials studied favor the elimination of the highly toxic and carcinogenic compounds generated in decomposition of 4-(Methylnitrosoamine)-1-(3-Pyrydyl)-1-Butanone, thus making them interesting materials for reducing of the toxicity of the tobacco smoke.

1. Introduction

Everyone knows that smoke can provoke cancer, and nicotine, present in cigarettes, causes the addiction to smoking. However, it is less known the amount of substances present in tobacco, or generated in the smoking process that can also cause cancerogenic effects [1–3]. Cigarette smoke includes more than 8000 different compounds [4], and it is likely that this number could still increase with further studies. At least 250 of such compounds are known to be harmful, including hydrogen cyanide, carbon monoxide, and ammonia. Moreover, 69 compounds have confirmed carcinogenic activity in humans [5,6].

Nicotine, a non-carcinogenic compound, is a member of the alkaloid family, and its amount in cigarettes is regulated and cannot exceed 1 mg per cigarette in EU [4,7]. When it is inhaled in cigarette smoke, it is absorbed into the bloodstream, and when it reaches the brain it stimulates the production of a number of neurotransmitters stimulating the production of dopamine, which is involved in human body's 'reward' pathways. This leads to the addictiveness of smoking.

Tobacco-specific nitrosamines (TSNAs) are one of the most important groups of carcinogens in tobacco products and there are principally formed by nitrosation of alkaloids present in the tobacco plant [8]. Normally, only a little portion of TSNA is generated during the smoke process; the major portion of the TSNA was generated during the curing process and transferred into tobacco smoke as preformed TSNA [9]. This can be seen by the fact that the smoke generated by cigarettes made with low tobacco in TSNA produces low yields of TSNA in the mainstream [10,11].

It has been shown that most of the nitrosamines cause mutations in DNA, and are carcinogenic to humans, being the nitrosamines 4-(Methylnitrosoamine)-1-(3-Pyrydyl)-1-Butanone (NNK; nitrosamine ketone derived from nicotine) and N-nitrosonornicotine (NNN) the ones with the highest risk [12,13]. It is generally accepted that NNN is formed via nitrosation of nornicotine, a secondary alkaloid generated directly from nicotine through the activity of the nicotine demethylase enzyme, and NNK is formed from nitrosation of nicotine or its oxidized products [14].

Zeolites and silicates are widely used for their catalytic properties, their ability to act as adsorbents, and their selectivity [15–20]. The use of zeolites and other mesoporous and microporous aluminosilicates as zeolite NaA, NaY, ZSM-5, SBA-15 and MCM-48, in the filter or directly

* Corresponding author. Inst. Univ. Ingeniería Procesos Químicos, Universidad de Alicante, 03080, Alicante, Spain.
E-mail address: antonio.marcilla@ua.es (A. Marcilla).

https://doi.org/10.1016/j.micromeso.2023.112571
Received 19 January 2023; Received in revised form 21 March 2023; Accepted 25 March 2023
Available online 29 March 2023

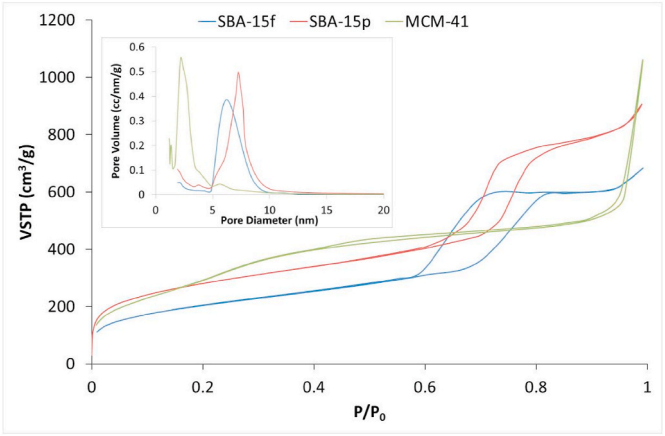

Fig. 1. N_2 adsorption isotherms and BJH pore size distribution calculated for the materials.

Table 1
Textural properties of mesoporous materials.

Material	Pore Size (nm)[a]	Tot Pore Vol (cm^3/g)[b]	BET Area (m^2/g)[c]
SBA-15f	6.1	0.97	728
SBA-15p	7.2	1.30	1009
MCM-41	2.2	1.51	1154

[a] Pore diameter BJH method applied to the desorption branch.
[b] Total pore volume at $P/P_0 = 0.99$.
[c] N_2 adsorption isotherms; BET theory.

mixed with tobacco, to reduce nitrosamines and polycyclic aromatics in the mainstream tobacco smoke has been described by several authors [21–23]. Our research group has been studying the effect of these type of materials mixed directly with tobacco for more than 10 years and has been able to demonstrate that addition of these materials in tobacco allows the reduction of the most of the compounds present in the mainstream tobacco smoke [24–28].

We have found no works that study the decomposition of nitrosamines when are heated, as well as the products generates during these processes. This fact becomes more important if we take into account that the habits of smokers are changing and new systems have emerged, such as HNB (Heat Not Burn) that permit to heat tobacco at low temperatures, between 250 and 300 °C [29–31]. On the other hand, in a typical cigarette coexist three types/zones of reactions, in the hot tip combustion reactions occur, that reach temperatures higher than 900 °C during the puff, reactions of pyrolysis appear in the area that is between the hot tip and the non-smoked tobacco where temperatures range around 300–600 °C, and a colder zone of non-smoked tobacco where the most volatile products are dragged out, as is the case of the TSNA [32].

In previous work we studied the effect of different materials, such as those used to reduce the tobacco smoke toxicity, on the thermal behavior of Nicotine [33] and NNN nitrosamine [34] under different atmospheres and temperatures. Nevertheless, the effect of such materials under such conditions, present in the smoking process, on NNK nitrosamine thermal behavior has not been studied. Thus, in this work, the decomposition of 4- methylnitrosamine-1,3-Pyrydiyl-1-Butanone (NNK) at three different temperatures has been analyzed in a TGA thermobalance and in a EGA equipment connected in line with a GC/MS to evaluate the nature of the compounds generated when this nitrosamine is heated, under inert and oxidizing atmosphere (He and air) emulating the processes of combustion and pyrolysis. In addition, the effect the effect of three mesoporous materials SBA-15f (fiber like morphology), SBA-15p (platelet like morphology) in direct contact with the NNK under the same conditions has been studied to evaluate the modification in the compound generated during the decomposition of this nitrosamine.

2. Experimental

2.1. Materials

Tobacco specific nitrosamine 4-(Methylnitrosoamine)-1-(3-pyridinyl)-1-butanone (NNK) 98+% was supplied from Alfa Aesar. SBA-15 with fibre like morphology (SBA-15f) was synthesized in our laboratory according the method reported in literature [35] where P123 (BASF) was dissolved in an acidic water using HCl 2 M (Merck 37%), and stirred at 38 °C during 1 h. Then TEOS (Wacker, >99% purity) was added to the mixture and kept at 40 °C under magnetic stirring 24 h, the resulting mixture was hydrothermally treated at 100 °C during 24 h. The final material was calcined at 550 °C during 6h. A SBA-15 with platelet morphology (SBA-15p), was synthesized according to the procedure described by Yeh et al. [36] using Cetyltrimethylammonium bromide and Sodium dodecyl sulphate (Acros Organics, >99% purity), sulphuric acid (Merck, >99% purity) sodium silicate (Schalau, neutral solution pure) and sodium hydroxide (Sigma Aldrich, >98% purity). The resulted material was calcined at 600 °C for 6 h in air for the removal of the organic templates. MCM-41 was synthetised as described Gaydhankar et al. [37] using Cetyltrimethylammonium bromide (Acros Organics, >99% purity), ammonia (merck, 25% solution) and Tetraethyl orthosilicate (Wacker, >99% purity), and the final material was obtained after calcined at 550 °C during 12 h. All the final materials were dried and stored in a desiccator to avoid water adsorption.

2.2. Characterization

The material was characterized by the N_2 adsorption isotherms at 77 K, measured in an automatic AUTOSORB-6 supplied by Quantachrome. The adsorption curves of the isotherms were recorded. The surface area was obtained by the Brunauer–Emmett–Teller (BET) method at relative pressure between 0.05 and 0.20 for SBA-15 materials, and 0.05–0.35 for MCM-41, and the pore size distribution was calculated from the

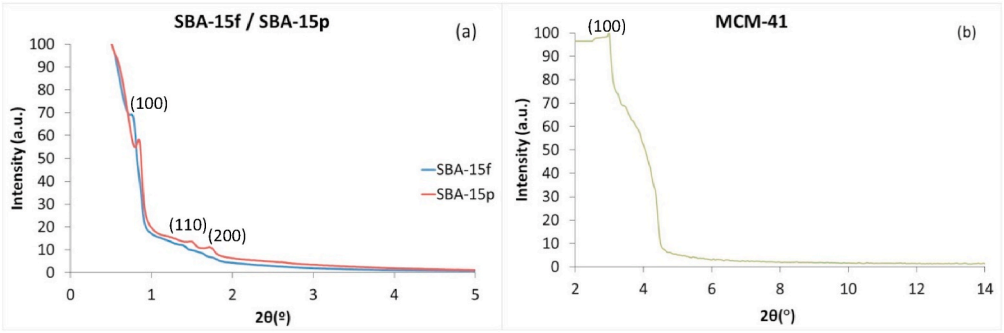

Fig. 2. *XRD d*ifractograms of the materials; a) SBA-15f and SBA-15p, b) MCM-41.

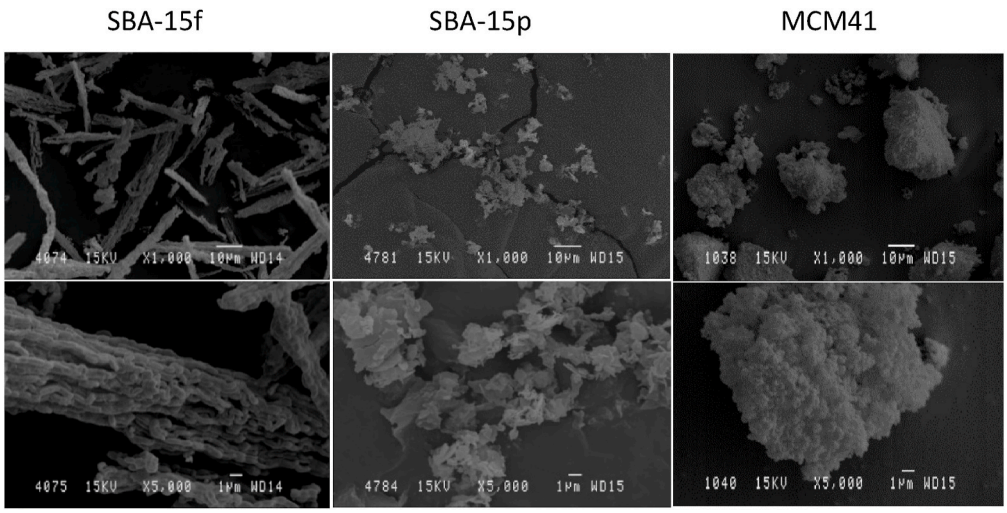

Fig. 3. SEM image of the catalyst.

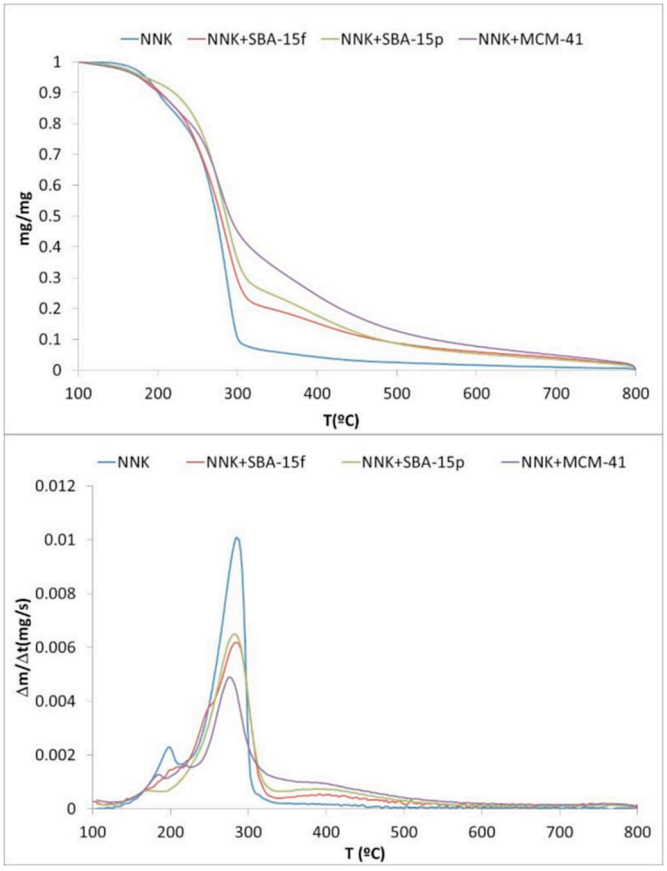

Fig. 4. TGA and DTG Curves of NNK and NNK + catalyst under inert atmosphere.

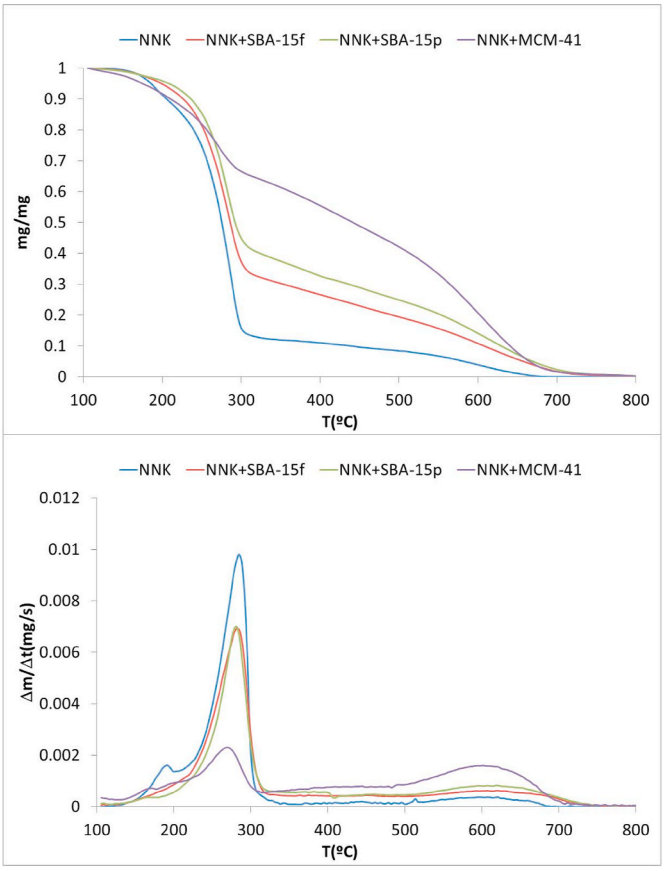

Fig. 5. TGA and DTG Curves of NNK and NNK + catalyst under oxidative atmosphere.

desorption branch of isotherm using the Barrett–Joyner–Halenda (BJH). The Pore Volume was calculated by the single point adsorption with the pores, less than 51. 4 nm diameter at $P/P_0 = 0.99$. Fig. 1 shows the N_2 isotherms and the pore size distribution of the materials, and Table 1 shows the textural properties of them. As can be seen, the MCM-41 isotherm shows an additional hysteresis loop of low significance at the highest P/P_0 value (0.90–0.99). This could indicate the presence of an unexpected secondary porosity in this material (may be due to particle coalescence). Fig. 2 show the XRD diffractograms of these materials. The equipment used for XRD is a Bruker D8-Advance with Göebel mirror with a KRISTALLOFLEX K 760-80F X-ray generator fitted with a copper anode X-ray tube. The two samples SBA-15 show the diffractogram peaks (100), (110) and (200) characteristic of the P6mm symmetry of these materials [38]. The diffraction pattern obtained for the MCM-41 material does not show the expected diffraction peaks, which could be related to the additional hysteresis cycle observed in N_2 adsorption and may be due to the coalescence of the particles. The morphology of the material was obtained by Scanning electron microscope (SEM) in a

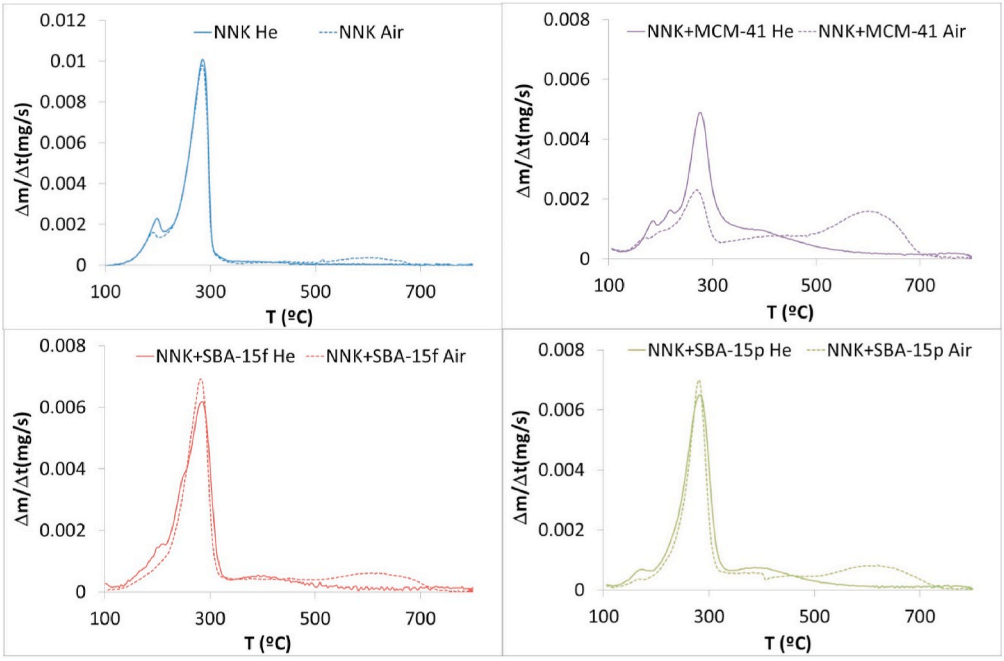

Fig. 6. Comparison between DTG curves obtained under inert and oxidative atmosphere.

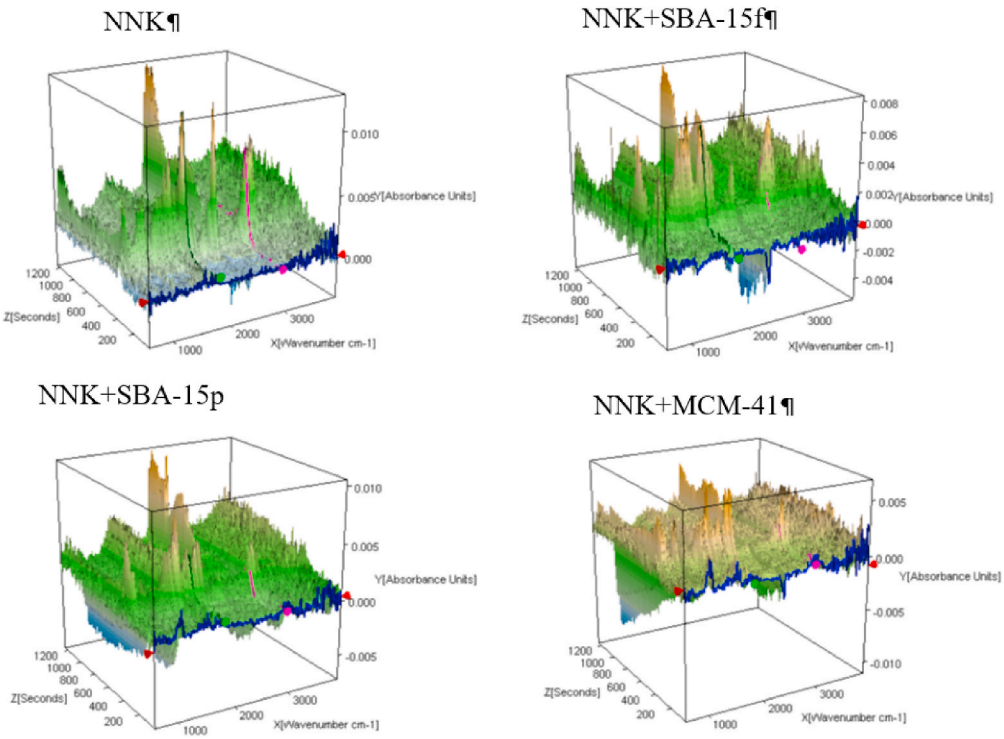

Fig. 7. 3D FTIR spectres obtained in the decomposition of NNK in inert atmosphere.

JSM-840 equipment and the micrographs of the three catalysts are shown in Fig. 3.

2.3. TGA and PY-GC/MS analysis

Thermogravimetric experiments (TGA) were conducted in a Mettler Toledo TGA/DSC 1 STARe Systems. The temperature program was 20 min at 40 °C, heating at 35 °C/min up to 800 °C and holding temperature during 5 min. 80 mL/min of N_2 (99.9992%) or air synthetic (21% O_2 and 79% N_2) where used as entrained gas in the corresponding experiments. For TGA experiments an initially 7–8% w/w solution of NNK in methanol was prepared. In the sample cup, 2 mg of the catalyst previously dried was introduced and then was added the necessary amount of the previous solution to guarantee the presence of 2 mg of NNK. The thermobalance is connected to a Bruker Tensor 27 FTIR spectrometer through a heated line (200 °C) which records the compounds generated in the TGA.

The flash decomposition were carried out using a multi-shot

Table 2
Assigned compounds under inert atmosphere at the different temperatures studied.

Compound	t_r (min)	Assignment	Match (%)
1	1.15	*CO_2*	**90**
2	1.12	Nitric oxide	**90**
3	1.17	Aziridine	**90**
4	1.18	Dimethyl ether	**90**
5	1.2	Methyl nitrite	**85**
6	1.23	Hydrocyanic acid	**95**
7	1.26	Ethanamine, N-methylene-	**80**
8	1.39	Acrolein	**97**
9	1.39	*Water*	**80**
10	2.02	*Propyl isocyanate*	**83**
11	2.85	*Acetonitrile, (dimethylamino)-*	**90**
12	2.85	*1,3-diazobicicle[3.1.0]hexane*	**91**
13	3.01	Pyridine	**91**
14	8.36	N-methylmaleimide	**91**
15	8.67	Pyridine, 3-ethyl-	**91**
16	8.83	Pyridine, 3-ethenyl-	**94**
17	9.57	4-pyridinecarboxyaldehyde	**93**
18	9.72	2-cyanopyridine	**90**
19	10.23	1-methyl-2-pyrrolidinone	**93**
20	11.37	3-acetylpyridine	**80**
21	11.84	Methyl nicotinate	**90**
22	11.86	3-hydroxypyridine	**91**
23	12.02	3-aminopyridine	**80**
24	12.58	1-(3-pyridinyl)-2-propen-1-one	-
25	12.76	1-(3-pyridinyl)-1-propanone	**80**
26	12.88	2-nitro-3-hydroxypyridine	**86**
27	13.7	Niacin	**95**
28	13.7	3-(4-pyridyl)acrylaldehyde	**84**
29	13.96	3-quinolinol	**85**
30	14.49	*Nicotine*	**81**
31	14.53	*1-isocyanate-4-methyl-Benzene*	**83**
32	15.29	Niacinamide	**94**
33	15.3	N-methylmyosmine	-
34	15.36	*Myosmine*	**95**
35	15.58	N-methyl-3-pyridinecarboxamide	**94**
36	15.74	3-propionylpyridine	**87**
37	15.8	2,6-dimethyl-3,4-dihydro-1,8-naphthyridine	-
38	16	*Nicotyrine*	**95**
39	16.45	3-(2,5-dimethyl-1H-pyrrol-1-yl)pyridine	-
40	16.85	Cyclopropyl-3-pyridinyl-methanone	**80**
41	17	3-(2,4-dimethyl-1H-pyrrol-1-yl)pyridine	-
42	17.31	Allyl nicotinate	**80**
43	17.43	4-hydroxy-7-methyl-1,8-naphthyridine	**80**
44	17.45	*(E)-4-(methylamine)-1-(pyridin*-3-yl*)but-2-en-1-one*	-
45	17.83	2,3-dihydro-5,8-dimethyl-1,4-naphthoquinone	**86**
46	18.55	*4,4'-(1,2-ethanedyl)bis-pyridine*	**80**
47	18.74	Phenyl nicotinate	**80**
48	19.34	(1-methyl-1H-imidazole-2-yl)2-pridinyl-methanone	**80**
49	20.28	*NNK*	**87**
50	24.74	4-methyl-1-(pyridin-2-yl)-1H-pyrrol-2-amine	-

pyrolyzer model EGA/PY-3030D supplied by FRONTIER LABORATORIES directly attached on a GC/MS from Agilent 6890 N gas chromatograph coupled in a Agilent 5973 inert mass selective detector. Helium gas was employed for experiments under inert atmosphere, and air synthetic for oxidative experiments. The samples, after purged with He in a cold chamber were dropped into the hot zone of the oven at the selected temperature. The heating rate in this mode of operation in the EGA/MS equipment is estimated in the range of hundreds of °C/S. UA5-30M-0.25F was used as a chromatographic column with a 2 ml/min flow oven programme used started at 45 °C during 5 min and temperature rise until 285 °C with a 12 °C/min rate ending with a 5 min isothermal at 285 °C, chromatograph inlet was at 300 °C and 50:1 split ratio. The mass spectrometer detector was equipped with an electron impact (EI) ion source at energy 70 eV, scan between 15 and 320 amu. In order to identify the products obtained on the chromatogram, NIST (National institute of standard and technology) library and Wiley library were used.

Initially, a 0.5% w/w solution of NNK in methanol was prepared. For the experiments in the EGA/PY, about 0.2 mg of the dried catalyst was introduced into the sample holder and 3.7 mg of the NNK solution was added to this bed. Prior to flash pyrolysis, a first in situ treatment was carried out in the equipment where the sample is heated at 80 °C for 4 min in an inert atmosphere, to remove the solvent (methanol).

Thermal study of the decomposition of NNK and NNK with catalysts was carried out in 2 atm at different temperatures. Flash pyrolysis experiments were done in He (99.9992% purity) between 300 and 500 °C at intervals of 100 °C. Flash oxidative experiments were performed in synthetic air (21% O_2 and 79% N_2) between 300 and 450 °C at intervals of 50 °C, due to the lower stability of NNK under oxidizing conditions, resulting in larger decomposition at lower temperatures. For the study of the effect of the three catalysts (SBA-15f, SBA-15p and MCM-41), three intermediate temperatures where selected, 300, 400, and 500 °C under inert atmospheres and 325, 375 and 425 °C under oxidative atmospheres. All experimenters were run by triplicate showing good reproducibility. Data reported correspond to the average of the three corresponding replicates.

3. Results and discusion

3.1. Thermogravimetric results

Fig. 4 shows the curves of loss weight (TGA) and its derivatives (DTG) obtained for NNK and its mixtures with the three catalysts in nitrogen atmosphere. The normalized weight fraction has been represented, calculated as the weight at each temperature minus the final weight divided by the initial weight minus the final weight. Data at temperature below 100 °C correspond to the volatilization of the solvent and the water present in the catalysts, and have been removed from the graphs.

As can be seen in the TGA and DTG curves, the decomposition of NNK exhibits three weight loss processes. The first observed at temperatures of the order of 202 °C, the main one, around 288 °C and a long tail at higher temperatures. When the NNK is mixed with the SBA-15f, the first process overlaps with the main process and practically disappears, the intensity of the main peak is reduced and the intensity of the last decomposition process of the residue increases. With the SBA-15p material, an initial process separated from the main one is again observed at a temperature of 175 °C, the intensity of the main peak is reduced and that of the last process increases. Finally, the presence of MCM-41 is the one that causes the greatest modifications. Two separate initial processes are observed, the intensity of the main process is greatly reduced and that of the last process is markedly increased. These facts may be related to the porous texture of these materials. MCM-41 has the largest BET area that seems to make its porosity more accessible to NNK and, although it has a smaller pore than SBA-15, it could be justified that it causes greater changes in the decomposition processes since it allows a greater interaction. This hypothesis could be confirmed by the fact that SBA-15p, which also has greater accessibility than SBA-15f, has an intermediate behavior between MCM-41 and SBA-15f.

Fig. 5 shows the results of TGA and DTG obtained in an air atmosphere. As can be seen, at temperatures below 350 °C, the behavior is very similar to that observed under inert atmosphere. Nevertheless, large changes are observed at higher temperatures. To better observe the different behavior between both atmospheres, Fig. 6 shows the DTG curves obtained for all the samples under the 2 atm tested.

In the decomposition of NNK, it can be observed that the presence of oxygen decreases the intensity of the first decomposition process, which occurs at somewhat lower temperatures, keeping the main process almost unchanged and increasing the residue of this first step, which decomposes at higher temperatures (500–680 °C). In the decomposition of NNK with SBA-15f, the first process decreases under inert atmosphere

Table 3
Contribution of the assigned compounds generated in the thermal decomposition of NNK to the total area (%) in both atmospheres at different temperatures (°C).

Compound	Inert atmosphere					Oxidative atmosphere						
	300	350	400	450	500	300	325	350	375	400	425	450
1	–	–	–	–	–	1.1	1.3	1.3	6.7	9.9	10.7	9.8
2	0.2	0.5	1.6	4.6	5.3	–	0.1	0.2	0.5	0.7	0.8	0.9
3	0.4	0.9	2.1	6.5	7.5	–	–	–	–	–	–	–
4	–	–	–	–	–	–	–	–	–	–	–	–
5	–	–	–	–	–	–	–	–	–	–	–	–
6	–	–	–	–	–	–	0.1	0.1	0.4	0.8	0.8	0.8
7	–	–	–	0.5	0.7	–	–	–	–	–	–	–
8	–	–	–	–	–	–	0.1	0.3	0.8	0.8	0.6	1.2
9	–	–	–	–	–	3.1	3.5	3.4	8.7	10.7	8.8	10.1
10	–	–	0.5	1.4	1.5	–	–	–	–	–	–	–
11	0.6	0.1	0.2	0.1	0.1	–	–	–	–	–	–	–
12	–	–	–	–	–	–	–	–	–	–	–	–
13	–	–	0.1	0.7	1	–	–	–	–	0.3	0.3	0.4
14	–	–	–	–	–	–	–	–	0.3	0.7	0.8	0.8
15	–	–	–	0.5	0.6	–	–	–	–	–	–	–
16	–	–	1.2	4.9	4.8	–	–	–	–	–	–	–
17	–	–	–	–	–	–	–	0.2	1.1	2.7	3.6	4.3
18	–	–	–	–	–	–	–	0.1	0.9	2.6	3.4	4.7
19	–	–	0.6	2.2	2.4	0.1	0.3	0.4	1.3	1.3	1.4	1.4
20	–	–	–	0.5	0.7	0.1	0.2	0.2	0.4	1.1	1.6	2
21	–	–	–	–	–	–	–	–	–	–	–	–
22	–	–	–	–	–	–	–	0.8	1.2	7	9.2	7.5
23	–	–	–	0.5	1.3	–	–	–	–	–	–	–
24	–	–	3.2	16.9	17.7	–	0.1	0.2	0.9	1.5	1.9	1.5
25	–	–	0.1	0.6	0.9	0.2	0.4	0.4	1.2	1.6	2.1	1.5
26	–	–	–	–	–	–	–	0.4	0.4	0.6	1.2	0.9
27	–	–	–	–	–	–	0.2	0.6	2.8	5.3	5.2	5.2
28	–	0.2	1.7	5.8	6.5	–	–	–	0.2	0.2	0.6	5.2
29	–	–	–	–	–	–	–	–	0.2	0.3	0.5	0.4
30	0.2	–	–	0.1	0.1	–	–	–	–	–	–	–
31	–	–	0.2	0.5	0.7	–	–	–	–	–	–	–
32	–	–	–	–	–	0.2	0.5	2.6	2.4	6	3.7	1.8
33	0.6	0.5	1.2	0.1	0.3	–	–	–	–	–	–	–
34	–	0.4	2.1	4.8	5.4	1.1	2	2.9	4.9	5.6	5.7	4.1
35	–	–	–	–	–	–	–	0.4	1.3	2.9	3.6	4.5
36	–	–	–	–	–	0.6	1.1	2.4	4.9	7.2	5.6	3.8
37	–	–	–	–	–	–	–	–	–	–	–	–
38	0.2	0.4	2	3.1	4.3	0.4	1	1.8	2.8	4.3	3.7	4.2
39	–	0.1	0.2	0.3	0.3	–	–	–	–	–	–	–
40	–	–	–	–	–	–	–	–	0.3	0.3	0.3	0.4
41	–	–	–	–	–	–	–	–	–	–	–	–
42	–	–	–	–	–	–	0.1	0.5	1.6	2.5	3.4	2.1
43	–	–	–	–	–	–	–	0.2	0.6	1.1	1.1	1.3
44	1	2.9	7.3	17.6	17.1	–	–	–	–	–	–	–
45	–	–	–	–	–	–	–	–	–	–	–	–
46	–	–	0.9	1.7	1.6	–	–	–	–	–	–	–
47	–	–	–	–	–	–	–	0.2	0.7	1.3	1.5	1.2
48	–	–	–	–	–	–	0.2	0.3	0.5	0.5	0.6	0.5
49	**96.7**	**90.5**	**64.2**	**10.6**	**-**	**93.05**	**85.9**	**75.3**	**39.4**	**3.2**	**-**	**-**
50	–	–	1.3	1.6	2.6	–	–	–	–	–	–	–

and disappears in the presence of oxygen. The main peak occurs in a narrower temperature range in the oxidizing atmosphere, and the proportion of residue increases and decomposes at higher temperatures. In the presence of SBA-15p, the peak corresponding to the first process is reduced in major proportion in the presence of oxygen, the main peak has a behavior analogous to that of SBA-15 f, and the residue that decomposes at high temperatures increases more markedly. Finally, the mixture of NNK with MCM-41 is the one that causes the greatest differences. As already mentioned, under inert atmosphere two processes appear at low temperatures. In an oxidizing atmosphere, these processes are greatly reduced, as well as the peak of the main decomposition stage, increasing the residue that decomposes at high temperatures (wide peak around 600 °C). In the presence of oxygen, as it happened under inert atmosphere, the MCM-41 material is the catalyst that causes the greatest modifications in the decomposition of NNK, followed by SBA-15p and SBA-15f. This effect can be due to the larger BET area and surface accessibility of MCM-41, despite the lower pore size as compared to of SBA-15, and seem to be large enough to enable its interaction with the NNK molecule. Another factor that may explain the lower effect of SBA-15 materials, that have larger pore size, is that within the channels part of the porosity is found as micropores. In addition, MCM-41 is a material with a high number of silanol groups on the external surface and on the inner surface of the pores that can generate acidity through hydrogen bonds that would be more accessible to NNK thus increasing its catalytic activity [18,39,40]. These silanol groups have the ability to interact with the N–NO group of NNK, retaining it inside the pores at low temperatures for its subsequent decomposition/elimination at higher temperatures.

Fig. 7 shows the 3D spectra obtained by FTIR in the NNK decomposition in the presence and absence of the materials used as a function of temperature. As can be seen, the spectra show poor resolution. Though the shape of the four spectra is very similar, these spectra show that the amount of compounds generated is reduced in the presence of the three materials, this reduction being greater in the presence of MCM-41. This would be in agreement with what was observed in TGA (Fig. 6) which showed that the MCM-41 was the material that most reduced the

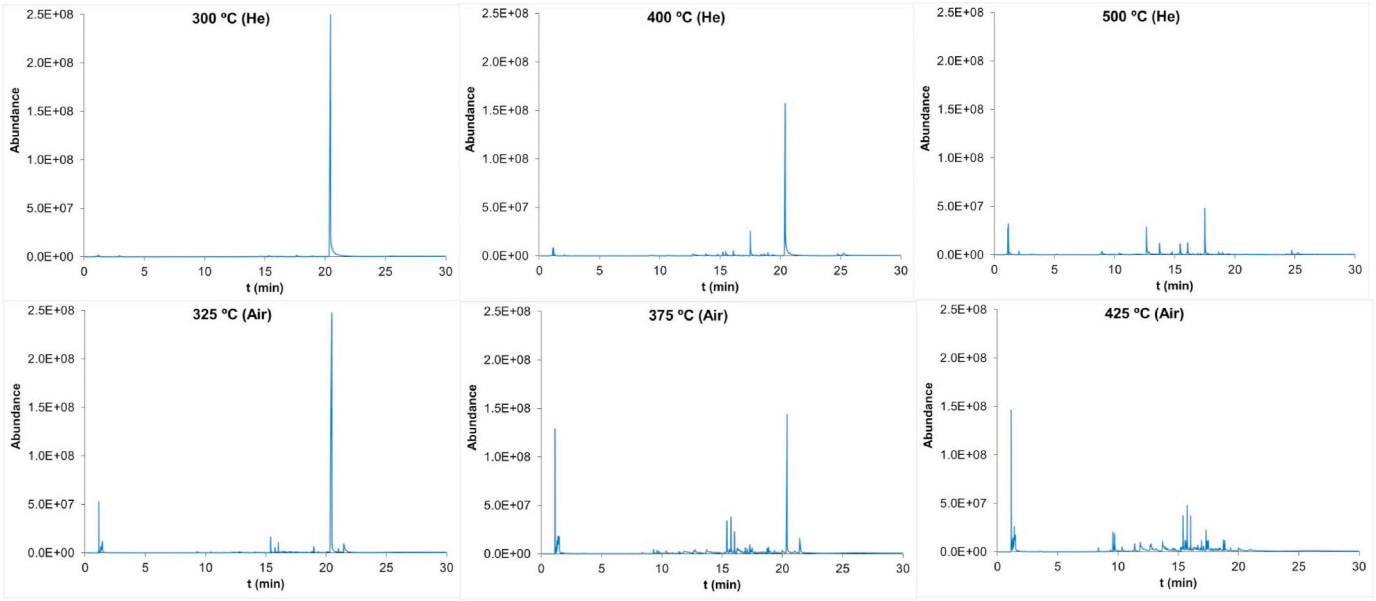

Fig. 8. Thermal chromatograms obtained at various temperatures in the decomposition of NNK at both atmospheres.

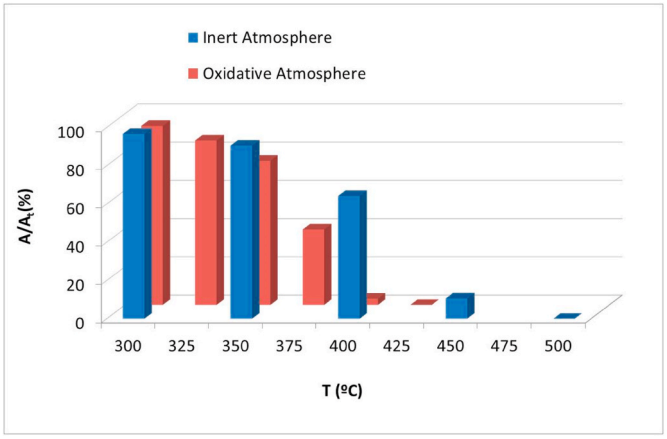

Fig. 9. Evolution of NNK with temperature in an inert and oxidizing atmosphere.

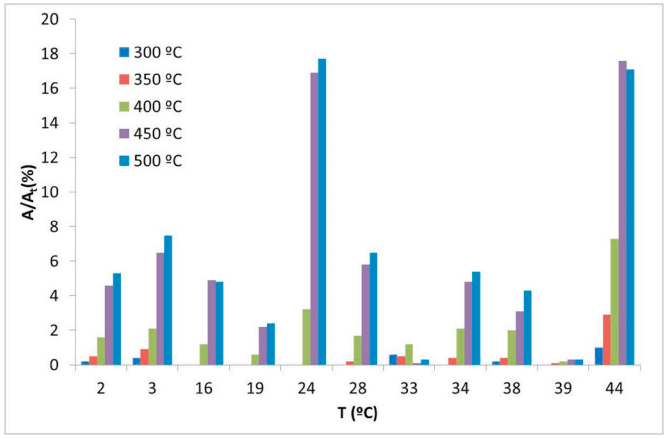

Fig. 10. Contribution to the total area (%) of the main compounds generated in the decomposition of NNK under inert atmosphere. *Nitric oxide (2), aziridine (3), 3-ethenyl-pyridine (16), 1-methyl-2-pyrrolidinone (19), 1-(3-pyridinyl)-2-propen-1-one (24), 3-(4-pyridyl)acrylaldehyde (28), N-methylmyosmine (33), myosmin (34), nicotyrine (38), 3-(2,5-dimethyl-1H-pyrrol-1-yl)pyridine (39), (E)-4-(methylamine)-1-(pyridin-3-yl)but-2-en-1-one (44).*

intensity of the main decomposition peaks (200–300 °C).

3.2. Flash decomposition of NNK

Five temperatures, between 300 and 500 °C, have been studied under inert atmosphere (pyrolysis) in the experiments run in the EGA Py/GC/MS equipment. These temperatures have selected to cover the decomposition temperature range of the NNK (i.e.: at 300 °C the 97% of the area of the chromatogram corresponds to NNK whereas at 500 °C no NNK was detected). Under oxidative atmosphere, the temperature range has been modified, since to 300 to 450 °C in increments of 50 °C. Under this atmosphere, the peak corresponding to NNK disappears at 425 °C and its contribution at 400 °C being only 3.2% of the total area (Table 3). In addition, the amount of compounds generated under this atmosphere is greater; the presence of oxygen promotes the degradation reactions yields a larger amount of compounds and a much more complex chromatogram.

Table 2 show the name of the compounds that present a contribution to the total area greater than 0.5% and in addition the coincidence with the spectrum in the library is greater than 80. Compounds that appear in the table without assigned probability are shown due to their relevance

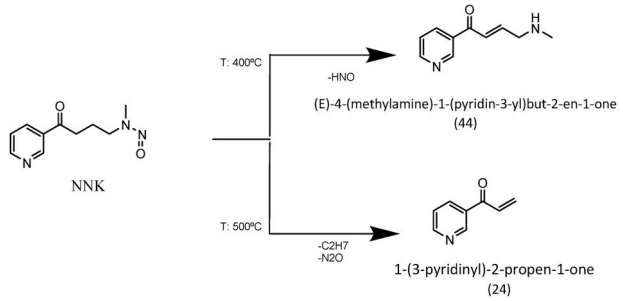

Fig. 11. Possible pathway for major NNK degradation compounds in inert atmosphere.

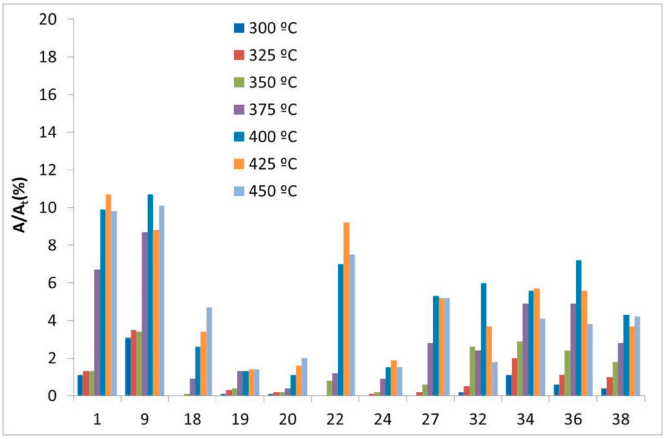

Fig. 12. Contribution to the total area (%) of the main compounds generated in the decomposition of NNK under air atmosphere. *Carbon Dioxide (1), Water (9), 2-Cyanopyridine (18), 1-Methyl-2-Pyrrolidinone (19), 3-Acetylpyridine (20), 3-Hydroxypyridine (22), 1-(3-Pyridinyl)-2-propen-1-one (24), niacin (27), niacinamide (32), myosmine (34), 3-propionylpyridine (36), nicotyrine (38).*

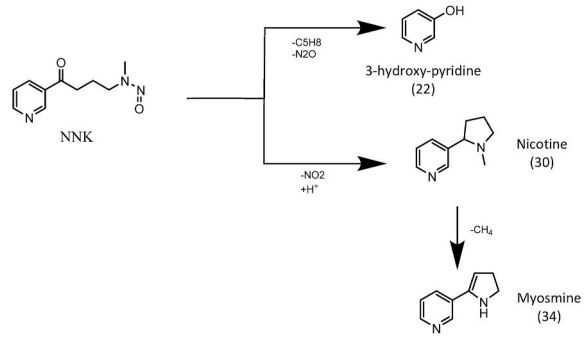

Fig. 13. Possible pathway for major NNK degradation compounds in air atmosphere.

in contributing to the total area, and were assigned manually from the mass spectrum obtained, considering the possible decomposition compounds of the NNK.

In the experiments under inert and oxidizing atmospheres, the different peaks obtained in the chromatogram have been integrated (A) and subsequently the areas obtained have been normalized with the total area (A_t) of the chromatogram to follow the contribution of each compound to the decomposition of NNK at the different temperatures studied. Table 3 shows the contributions to the total area of the assigned compounds in the pyrolysis of NNK under inert and oxidizing atmosphere.

Fig. 8 shows, as example, the chromatograms obtained for the decomposition of the NNK under inert atmosphere (He) and oxidative atmosphere (Air) at three temperatures. As can be seen at low temperatures the peak of NNK (20.28 min) is the principal, and when the temperature increase, this peak decreases and more new peaks appear. This tendency is similar in both atmospheres.

Fig. 9 shows the contribution of the NNK to the total area of the corresponding chromatogram as a function of temperature, for both atmospheres. As can be seen, at low temperatures (300 °C) the NNK practically not decomposes, since its contribution to the total area greater than 90% in both atmospheres, and higher under inert atmosphere (Table 3). Also, the degradation of NNK occurs much faster under oxidizing atmosphere, and at 400 °C practically no NNK appears in the chromatogram (3.2% in air versus 64.2% in He). Under inert atmosphere at 450 °C its contribution is still 10.6% and it is necessary to reach 500 °C for eliminate it completely.

Fig. 10 shows the area percentage of the most important decomposition compounds obtained in the NNK pyrolysis experiments under inert atmosphere. It can be seen that all the compounds increase their contribution when increasing the temperature, so it follows that they are formed as a consequence of the pyrolytic decomposition suffered by NNK. At 300 °C, more than 96% of the total area of the chromatogram is due to NNK, but a small part begins to decompose, giving rise to the appearance of some high molecular weight compounds, such as (E)-4-(methylamine)-1-(pyridin-3-yl)but-2-en-1-one (44). At 400 °C, an increase in the amount of compounds generated is observed, being the major again the compound 44, with 7.3% of the total area. However, at 500 °C, when all the NNK has decomposed, this compound represents 17.1% of the total area and the formation of 1-(3-pyridinyl)-2-propen-1-one (24) is favored, which it represents 17.7% of the total area. This results show that compound 44 decomposes at high temperatures.

According to the works Lin et al. and Miura et al. [21,41], the N–NO group of the NNK is the most reactive of this molecule and is where the pyrolytic rupture begins. Lin et al. [21] studied the decomposition thermal and catalytic of NNN nitrosamine. These authors found two major products due to spontaneous pyrolysis of this nitrosamine. The first was formed by the loss of the nitrous group since the N–NO bond has the weakest binding energy in the nitrosamine molecule. And it stabilizes with the reduction of the molecule with the loss of hydrogen to form a double bond. In this work we have observed the same tendency, and at 400 °C the NNK is transformed into a secondary amine, losing the nitrous group and forming a double bond in the hydrocarbon chain leading the formation of (E)-4-(methylamine)-1-(pyridin-3-yl)but-2-en-1-one (compound 44) (Fig. 11). In addition, Lin et al. [21] also observed that this major product was unstable at higher temperatures, where the rupture of the chain attached to the pyridine ring led to the formation of a new compound. This behaviour is also observed in the pyrolysis of NNK, where at higher temperatures the amount of compound (44) decreases and a α, β-unsaturated compound such as 1-(3-pyridinyl)-2-propen-1-one (24), is generated as the main compound.

Fig. 12 shows the main NNK decomposition compounds in an oxidizing atmosphere. As can be seen, at low temperatures, 300 and 325 °C, the decomposition of NNK mainly produces carbon dioxide (1) and water (9), and other compounds begin to be generated in small amounts, being myosmin one of the most abundant (34). At 375 °C, more than half of the NNK has been degraded (Table 3), and CO_2 (1) and H_2O (9) are the main products, but 3-propionylpyridine (36) is generated in the same proportion as myosmin (34), and other compounds also appear in notable proportions such as nicotyrine (38), niacin (27), niacinamide (32) and 1-(3-pyridinyl)-2-propen-1-one (24). At 425 °C, NNK has been completely degraded and, together with CO_2 (1) and H_2O (9), 3-hydroxypyridine (22) appears as the main compound, representing 9.2% of the total area. This compound is not formed during pyrolysis in an inert atmosphere, so its generation is conditioned by the presence of oxygen. Fig. 13 shows the possible route for obtaining the major NNK degradation compounds (i.e.: compounds 22 and 34) in an oxidizing atmosphere. In this atmosphere, due the high reactivity of oxygen, and with high temperatures, the pyridine ring can loss the group N–NO and the rest of the chain forming 3-hydroxypyridine (compound 22) as the principal compound. At lower temperatures, the internal cyclization of the chain is favored, giving raise to different compounds derivatives of nicotine, such as myosmin (compound 34).

When comparing the results obtained in both atmospheres, some common compounds can be observed, such as 1-methyl-2-pyrrolidinone (19), 1-(3-pyridinyl)-2-propen-1-one (24), myosmine (34), and nicotyrine (38), but with clear differences in distribution. Thus, myosmine (34) is favored in an oxidizing atmosphere, and for example 1-(3-pyridinyl)-2-propen-1-one (24), is highly favored in an inert atmosphere with 17.7% of the total area.

Table 4
Contribution of the assigned compounds generated in the catalytic decomposition of NNK to the total area (%) in both atmospheres at different temperatures (°C).

	Inert Atmosphere									Oxidative Atmosphere								
	NNK + SBA-15f			NNK + SBA-15p			NNK + MCM-41			NNK + SBA-15f			NNK + SBA-15p			NNK + MCM-41		
	300	400	500	300	400	500	300	400	500	*325*	*375*	*425*	*325*	*375*	*425*	*325*	*375*	*425*
1	–	–	–	–	–	–	–	–	–	1.1	5.1	7.8	1.8	9.1	12.5	3.6	12.9	19.2
2	0.2	1.7	3.3	0.3	1.7	3.5	3.9	7.1	17	0.3	0.9	1.2	0.4	1.8	2	0.4	0.5	0.4
3	0.2	1	3.3	0.2	0.6	2.4	–	1.2	6	–	–	–	–	–	–	–	–	–
4	–	–	–	–	–	–	–	–	–	–	–	–	–	–	–	1.3	1.5	3.1
5	–	–	–	–	–	–	–	–	–	–	–	–	–	–	–	–	2	2.4
6	–	–	–	–	–	–	–	–	–	–	0.1	0.2	–	0.2	0.1	–	–	–
7	–	0.4	0.7	–	0.5	0.4	–	–	–	–	–	–	–	–	–	–	–	–
8	–	–	–	–	–	–	–	–	–	0.4	1.2	1.6	–	2.3	1.7	0.7	1.1	1.1
9	–	–	–	–	–	–	–	–	–	5.7	9.3	11.5	10.6	22.3	17	10.3	23.6	31.4
10	–	0.2	0.5	–	0.1	0.4	–	0.3	0.9	–	–	–	–	–	–	–	–	–
11	0.2	0.1	0.2	0.8	0.3	0.2	0.8	1.4	1	–	–	–	–	–	–	–	–	–
12	–	–	–	–	–	–	–	–	–	–	–	–	–	–	–	0.9	0.7	0.2
13	–	–	0.6	–	–	0.4	–	–	3.2	–	–	0.8	–	–	0.5	0.2	0.9	1.3
14	–	–	–	–	–	–	–	–	–	–	–	1.2	–	–	0.3	–	–	0.3
15	–	–	0.2	–	–	0.2	–	–	–	–	–	–	–	–	–	–	–	–
16	–	–	1.7	–	–	1.1	–	–	1.7	–	–	–	–	–	–	–	–	–
17	–	–	–	–	–	–	–	–	–	–	0.3	1.9	–	–	1.3	–	0.4	1.2
18	–	–	–	–	–	–	–	–	–	–	2.4	7.2	–	1.5	6.9	–	1.4	3.7
19	–	0.3	1	–	0.3	0.8	–	–	–	–	0.9	1.1	–	0.4	1.4	–	0.7	1.1
20	–	0.5	1.3	–	0.5	1.4	–	–	2	–	0.9	1.7	–	0.8	1.7	–	0.5	1.4
21	–	–	–	–	–	–	–	–	–	–	1.3	1.1	–	0.6	0.5	–	0.5	0.4
22	–	–	–	–	–	–	–	–	–	–	0.7	1.4	–	–	1.3	–	–	1.1
23	–	–	–	–	–	–	–	–	–	–	–	–	–	–	–	–	–	–
24	–	–	7.5	–	–	4.3	–	–	2.6	–	0.6	1.7	–	1.6	1.8	–	0.4	4
25	–	0.9	0.5	–	0.6	0.5	–	–	5	–	2.3	2.1	–	–	3	–	1.1	–
26	–	–	–	–	–	–	–	–	–	–	–	–	–	–	–	–	–	–
27	–	–	–	–	–	–	–	–	–	–	–	–	–	–	–	–	–	–
28	–	0.6	3.1	–	0.4	2.2	–	–	3.4	–	–	0.4	–	–	0.5	–	–	0.4
29	–	–	–	–	–	–	–	–	–	–	–	–	–	–	0.4	–	–	0.6
30	–	0.2	0.2	0.4	1.4	1.1	–	0.4	0.4	–	–	–	–	–	–	–	–	–
31	–	–	0.3	–	–	0.2	–	–	–	–	–	–	–	–	–	–	–	–
32	–	–	–	–	–	–	–	–	–	–	–	–	–	–	–	–	–	–
33	3	1.3	0.3	1.4	1.2	–	2.4	13.9	2.7	–	–	–	–	–	–	–	–	–
34	3.7	9.1	9.2	2.7	9.3	9.8	–	3.3	5.3	1.5	5.7	6.7	1.5	5.7	5.3	0.5	2	1.5
35	–	–	–	–	–	–	–	–	–	–	0.4	1.9	–	0.3	0.8	–	0.4	1.1
36	–	–	–	–	–	–	–	–	–	–	2.7	4.2	–	0.8	4.5	–	2.9	2.9
37	1.1	1.9	1.5	1.4	2.8	2.6	–	0.8	1.1	–	–	–	–	–	–	–	–	–
38	11.1	20.7	24.8	8.3	17.8	23.3	1.2	10.5	22.9	2	14.1	24.9	1.9	16.2	16.4	1.7	3.3	3.6
39	6.1	12.6	13.3	7.3	18.8	24	0.4	4.2	11.9	–	0.6	1.2	–	1.3	1	–	–	0.2
40	–	–	–	–	–	–	–	–	–	–	–	0.2	–	–	0.2	–	–	0.1
41	1.9	4.4	4.8	1.2	6.8	8.3	–	–	1.1	–	–	–	–	–	–	–	–	–
42	–	–	–	–	–	–	–	–	–	–	–	0.7	–	–	1.3	–	–	–
43	–	–	–	–	–	–	–	–	–	–	0.3	0.4	–	–	0.5	–	–	–
44	0.7	4.2	10.3	0.4	2.2	6.2	–	2.4	5.4	–	–	–	–	–	–	–	–	–
45	–	–	–	–	–	–	–	–	–	–	0.3	0.6	–	0.5	0.6	–	–	–
46	–	0.1	1.1	–	0.3	0.3	–	–	–	–	–	–	–	–	–	–	–	–
47	–	–	–	–	–	–	–	–	–	0.1	0.3	0.6	–	–	0.4	1	0.4	0.8
48	–	–	–	–	–	–	–	–	–	0.3	1.9	2.1	1.3	6.3	4.9	2.4	7.9	5.8
49	**70.5**	**34.4**	**-**	**73.4**	**27.8**	**-**	**91.3**	**47.1**	**-**	**85.7**	**40**	**-**	**79**	**18.4**	**-**	**75.6**	**23.8**	**-**
50	–	–	0.7	–	–	–	–	2	3	–	–	–	–	–	–	–	–	–

3.3. Catalytic decomposition of NNK

During the catalytic experiments under inert atmosphere (pyrolysis), three temperatures have been studied for the decomposition of NNK in presence of the three materials, 300, 400 and 500 °C and 325, 375 and 425 °C under oxidative atmosphere. Table 4 shows the compounds obtained in the catalytic decomposition of the NNK that present a contribution to the total area greater than 0.5% and, in addition, present an assignment with a probability greater than 80%, in both atmospheres, at the studied temperatures. As can be seen in Fig. 14 and Table 4, at low temperatures, in presence of the catalyst more degradation of NNK can be observed. At 300 °C in the thermal decomposition, the area that represents the NNK peak is greater than 96%, in the presence of MCM-41 it drops a little to 91.3% and with SBA-15p it drops to 73.4% and SBA-15p shows the highest decomposition values, 70.5% (Table 4). At 400 °C, the material that shows a major decomposition of the NNK is SBA-15p, followed by SBA-15f, and again, MCM-41 is the material that least affects the NNK. At 500 °C, as in thermal decomposition, the NNK is completely decomposed. These results agree with what was observed by Zhu et al. [42]. These authors concluded that the presence of SBA-15 type silicates reduces the presence of NNK in tobacco smoke and favors the thermal degradation of this molecule previously adsorbed on SBA-15 [43–45].

Fig. 15 shows the contributions to the total area of the main NNK decomposition compounds in the presence of the studied catalysts, under inert atmosphere as a function of temperature. Between 300 °C and 400 °C, with the three catalysts, an increase in the generation of decomposition compounds can be observed as a function of temperature, which corresponds to the reduction in the amount of NNK decomposed. Lin et al. [21] highlighted the ability of SBA-15, MCM-41 and various zeolites as NaY to remove both total particulate matter and TSNAs in tobacco smoke, and the decomposition of NNN directly deposited on the catalysts. Lin et al. observed that the materials MCM-41 and SBA-15 were the ones that most reduced TPM (19% MCM-41 and

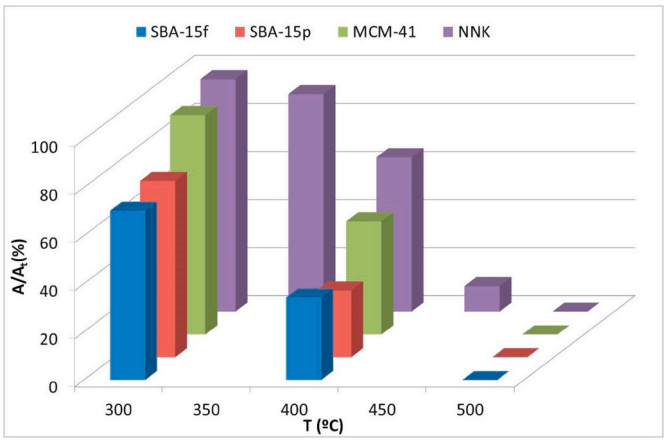

Fig. 14. Decomposition of NNK in presence and absence of catalyst under inert atmosphere.

30% SBA-15) and TSNA (22% MCM-41 and S35% BA-15), but not important modification in the products obtained with SBA-15 and MCM-41 was observed. In this work, GC/MS experiments show that the main compounds identified in the catalytic pyrolysis are the same as those obtained in NNK thermal pyrolysis, but their distribution is different. The presence of the two SBA-15 favors the formation of compounds with higher molecular weight, especially myosmin (34), nicotyrine (38) and 3-(2,5-dimethyl-1H-pyrrol-1-yl) pyridine (39). Compound 39 is practically not generated in the experiments in the absence of mesoporous silicates and furthermore the SBA-15 materials reduce more than halve the formation of (E)-4-(methylamine)-1-(pyridin-3-yl) but-2-en-1-one (44), one of the heaviest compounds generated in thermal decomposition. It can be due to the high pore size of these materials, which allow NNK to be retained long enough to favor the cyclization of the pyridine ring chain favoring the formation of myosmin (34), nicotyrine (38) and 3-(2,5-dimethyl-1H-pyrrol-1-yl) pyridine (39).

If we compare both materials, SBA-15f catalyst favors the formation of nicotyrine (38), while SBA-15p, that shows higher BET area and pore size favors somewhat the formation of compound 39 and also shows a large amount of compound 38. On the other hand, both SBA-15 materials reduce the formation of lower molecular weight compounds such as NO (2), aziridine (3), 3-ethenyl-pyridine (16) and 1-(3-pyridinyl)-2-propen -1-one (24) among others, being especially notable the case of compound (24), which at 500 °C is mainly generated in the thermal decomposition, while for catalytic pyrolysis it has a minor contribution.

MCM-41 also shows an increase in the compounds but to a lesser extent and considerably reduces the formation of 3-ethenyl-pyridine (16), 1-methyl-2-pyrrolidinone (19), 1-(3-pyridinyl) -2-propen-1-one (24) and 3-(4-pyridyl) acrylaldehyde (28), highlighting the practical disappearance of compound 24. This catalyst, unlike the two SBA-15

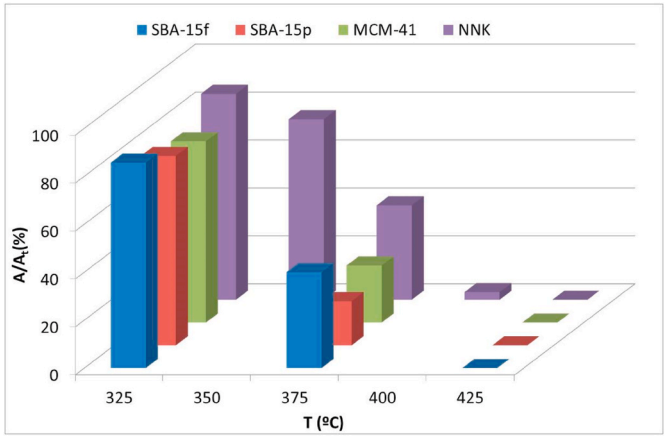

Fig. 16. Decomposition of NNK in presence and absence of catalyst under oxidative atmosphere.

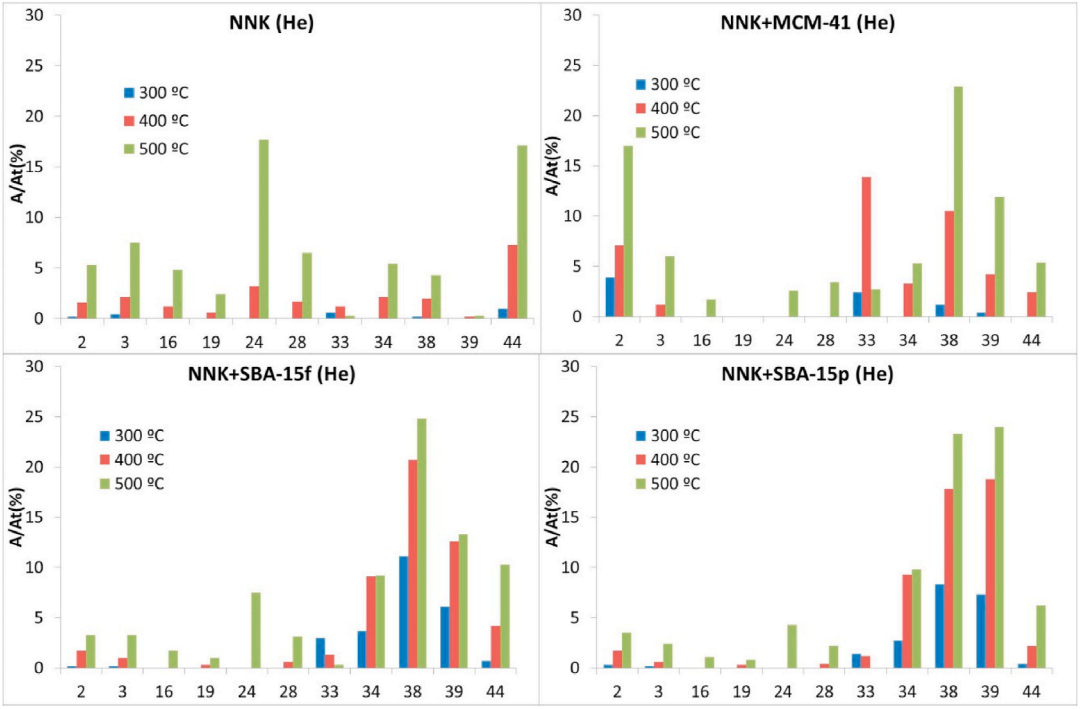

Fig. 15. Contribution to the total area (%) of the main compounds generated in the thermal and catalytic decomposition of NNK, under inert atmosphere. Nitric oxide (2), aziridine (3), 3-ethenyl-pyridine (16), 1-methyl-2-pyrrolidinone (19), 1-(3-pyridinyl)-2-propen-1-one (24), 3-(4-pyridyl)acrylaldehyde (28), N-methyl-myosmine (33), myosmin (34), nicotyrine (38), 3-(2,5-dimethyl-1H-pyrrol-1-yl)pyridine (39), (E)-4-(methylamine)-1-(pyridin-3-yl)but-2-en-1-one (44).

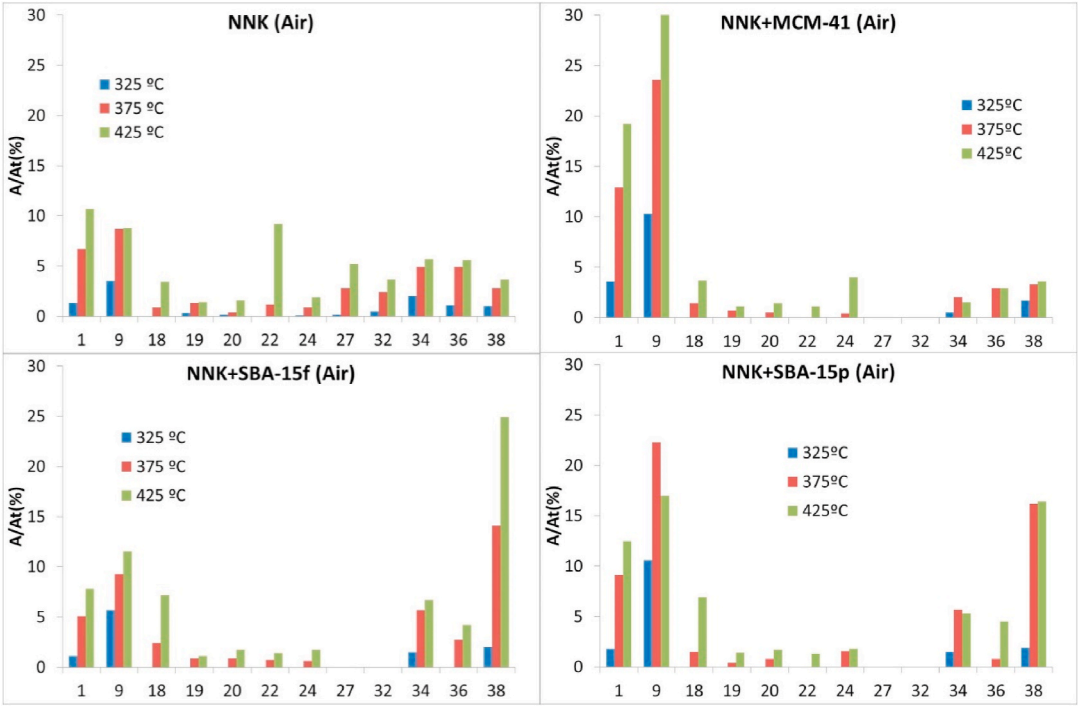

Fig. 17. Contribution to the total area (%) of the main compounds generated in in the thermal and catalytic the decomposition of NNK under inert atmosphere. *Carbon Dioxide (1), Water (9), 2-Cyanopyridine (18), 1-Methyl-2-Pyrrolidinone (19), 3-Acetylpyridine (20), 3-Hydroxypyridine (22), 1-(3-Pyridinyl)-2-propen-1-one (24), niacin (27), niacinamide (32), myosmine (34), 3-propionylpyridine (36), nicotyrine (38).*

Table 5
Toxic compounds present in the gases generated in the decomposition of NNK.

		SBA-15f		SBA-15p		MCM-41	
		He	Air	He	Air	He	Air
3	***Aziridine***	↓	-	↓	-	↓	-
6	***Hydrocyanic acid***	-	↓	-	↓	-	↓
7	***N-methylenethanamine***	↑	-	↓	-	↓	-
8	***Acroleine***	-	↑	-	↑	-	↑
13	***Pyridine***	↓	↑	↓	↑	↑	↑
16	***3-ethenyl-Pyridine***	↓	-	↓	-	↓	-
30	***Nicotine***	↑	-	↑	-	↑	-
49	***NNK***	↓	↓	↓	↓	↓	↓

materials, greatly favors the formation of N- methylmyosmine (33) at 400 °C, and nitric oxide (2) as the decomposition temperature increases.

Fig. 16 shows the contribution to the total area of the NNK as a function of the temperature in the oxidizing atmosphere, for pure NNK and for the mixtures of NNK + catalyst. As can be seen, the SBA-15f catalyst in an oxidizing atmosphere practically does not affect the degradation of the NNK, keeping its contribution to the total area similar to that obtained in the thermal experiments. On the other hand, the SBA-15p shows a little decrease in the contribution to the total area NNK compared to the experiment without catalyst at 325 °C (85.7% for NNK vs 79% for NNF + SBA-15p) that increases when temperature increases, observing a reduction at 375 °C from 40% for pure NNK to 18.4% for NNK + SBA-15p. MCM-41 is the material that shows the major reduction at 325 °C, although it is very small, and at 375 °C it shows an intermediate behavior between both SBA-15.

In Fig. 17, the contributions to the total area of the main decomposition compounds studied for oxidizing conditions are represented. The results show how the presence of SBA-15 catalysts notably favors the formation of nicotyrine (38), a nitrogenous alkaloid, going from 3.7% at 425 °C in the thermal decomposition, to 25% in the experiments with SBA-15f and 16.4% with SBA-15p. In the presence of MCM-41, this effect is not observed, compound 38 maintaining a percentage similar to the experiment without catalyst. This could be due to the fact that the SBA-15 have a large pore size that allows the retention of the NNK for the time necessary to cycle the ring chain, but the MCM-41 material, which has a greater number of silanol groups and favors the complete catalytic decomposition of these products with the consequent increase in the formation of carbon dioxide (1) and water (9). However, the use of catalysts favors the reduction of some compounds formed by the decomposition of NNK in an oxidizing atmosphere, such as 3-hydroxypyridine (22). In addition, compounds such as niacin (27) and niacinamide (32) are not formed in the presence of these catalysts, so they can be considered to be products of the thermal oxidation of NNK.

From these results it can be deduced that the presence of these materials favors the oxidation of NNK, especially the SBA-15p, which has a more accessible porosity and increases the formation of oxidative degradation compounds such as compounds 1 and 9, in addition to favor the selective formation of nicotyrine (38), a selectivity that does not occur in the MCM-41 material due to its smaller pore size.

Finally, the data obtained can be analyzed from the point of view of the toxicity. The NNK is a highly carcinogenic substance cataloged by the IARC in group 1 [46]. The studied catalysts favor the degradation of this compound and also modify the composition of the gases generated. From the list of compounds studied in this chapter collected in Table 2, the toxic and dangerous compounds for humans present in tobacco smoke have been selected based on the data published in different bibliographic sources [47–49]. Table 5 shows these compounds as well as the variation they undergo in the presence of mesoporous silicates.

As can be seen, the three materials practically show the same variation increasing or reducing the contribution to the area of each of the toxic compounds. The three materials in He atmosphere reduce aziridine, 3-ethenyl-pyridine and, as mentioned, NNK, while increasing nicotine. N-methylenethanamine increases with SBA-15f but decreases in the presence of the other two materials, and pyridine decreases in the presence of both SBA-15 and increases with MCM-41. Furthermore, neither hydrogen cyanide nor acrolein is formed in the presence of the catalysts under inert atmosphere. In addition, these materials under air

atmosphere reduce hydrogen cyanide and obviously NNK, while increasing acrolein and pyridine. In this atmosphere, aziridine, N-methylenethanamine, 3-ethenyl-pyridine and nicotine are not generated.

4. Conclusions

TGA experiments show that NNK degradation exhibits several processes of decomposition showing a slight influence of the atmosphere used. When mesoporous silicates are introduced, important variations are observed in the thermal processes due to adsorption and/or catalysis processes. This variation is more notable in air atmosphere where a process at high temperatures is observed due to the generation of CO_2 and CO when the remaining residue is burned. MCM-41 is the material that generates the most significant changes in the decomposition of NNK, probably due to its larger BET area and surface accessibility, despite the lower pore size as compared to SBA-15, it seems to be large enough to enable the interaction with the NNK molecule. The micro porosity interconnecting the walls of mesopores in the SBA-15 may be not accessible to the NNK molecule which may also contribute to the lower activity as compared to MCM-41. The final residues obtained are always larger in the presence of catalysts, being larger under inert atmosphere, showing the ability of the catalysts to favor coke formation.

In EGA experiments it has been possible to monitor the composition of the gases generated as a function of temperature. The composition of the gas generated in an inert atmosphere is mainly composed of 1-(3-pyridinyl)-2-propen-1-one (24), myosmine (34) and (E)-4-(methylamine)-1-(pyridin-3-yl)but-2-en-1-one (44) and by 3-hydroxypyridine (22), myosmine (34) and 3-propionylpyridine (36) in addition to CO_2 (1) and H_2O (9) in atmosphere oxidizing. In the presence of mesoporous silicates the compounds generated are modified. All three materials accelerate the decomposition of NNK in both atmospheres. Under inert atmosphere, MCM-41 followed by SBA-15p are the materials that show the larger changes in the composition of the main gases generated and advance the degradation of NNK. For example, the catalysts decrease the formation of the main compounds obtained in the decomposition of NNK, 1-(3-pyridinyl)-2-propen-1-one (24) and (E)-4-(methylamino)-1-(pyridin-3-yl)but-2-en-1-one (44) and favor the formation of Nicotyrine (38).

Under oxidizing atmosphere, the degradation is also advanced at lower temperatures and the generation of CO_2 (1), H_2O (9) and nicotyrine (38) increases. The presence of the catalyst reduces the formation of principal compounds as 3-hydroxypyridine (22) and myosmine (34), specially the MCM-41 and eliminate completely compounds as Niacin (27) and 3-(4-pyridyl)acrylaldehyde (26).

In conclusion, NNK is known to be one of the most carcinogenic compounds for humans present in tobacco. The use of these catalysts has shown to favor its degradation yielding lower amounts of toxic products and, therefore, making them interesting materials from the point of view of reducing the toxicity of tobacco smoke.

Funding

Financial support for this investigation has been provided by the “Conselleria de Educacion, Investigacion, Cultura y Deportes” (IDIFEDER 2018/009 and PROMETEO 2020/093).

CRediT authorship contribution statement

J. Asensio: Visualization, Validation, Methodology, Investigation, Data curation. **M.I. Beltran:** Supervision, Methodology, Conceptualization. **A. Marcilla:** Writing – review & editing, Supervision, Project administration, Methodology, Conceptualization. **D. Berenguer:** Writing – original draft.

Declaration of competing interest

The authors declare that they have no known competing financial interests or personal relationships that could have appeared to influence the work reported in this paper.

Data availability

No data was used for the research described in the article.

References

[1] D. Hoffmann, I. Hoffmann, Beitr. Tabaksforsch. Int. 18 (1998) 49–52, https://doi.org/10.2478/cttr-2013-0678.
[2] A. Thielen, H. Klus, L. Muller, Exp. Toxicol. Pathol. 60 (2008) 141–156, https://doi.org/10.1016/j.etp.2008.01.014.
[3] M. Borgerding, H. Klus, Exp. Toxicol. Pathol. 57 (2005) 43–73, https://doi.org/10.1016/j.etp.2005.05.010.
[4] S.H. Stephen, E. Szabo, Cancer Prev. Res. 7 (1) (2014) 1–8, https://doi.org/10.1158/1940-6207.CAPR-13-0371.
[5] U.S. Department of Health and Human Services, The Health Consequences of Smoking—50 Years of Progress: A Report of the Surgeon General, 2014, U.S. Department of Health and Human Services, Centers for Disease Control and Prevention, National Center for Chronic Disease Prevention and Health Promotion, Office on Smoking and Health, Atlanta, GA, 2014.
[6] National Toxicology Program, Tobacco-related exposures, in: Report on Carcinogens, fourteenth ed., U.S. Department of Health and Human Services, Public Health Service, National Toxicology Program, 2016.
[7] Directive 2014/40/eu of the European Parliament and of the Council, Official Journal of the European Union, 2014. L 127/13.
[8] S.H. Stephen, Metabolism of Carcinogenic Tobacco-specific Nitrosamines, National Cancer Institute, 2004.
[9] S. Fischer, B. Spiegelhalder, J. Eisenbarth, R. Preussmann, Carcinogenesis 11 (5) (1990) 723–730, https://doi.org/10.1093/carcin/11.5.723.
[10] D.M. Peele, D.A. Danehower, G.D. Coins, Coresta Information Bulletin. Chemical and Biochemical Changes during the Flue-Curing of Tobacco, 1995.
[11] D.J. Doolittle, J.T. Avalos, B.R. Bombick, K.P. Putnam, T.B. Nestor, J.S. Gentry. Tox Sci. 60 (2001) 416–425, https://doi.org/10.1093/toxsci/60.2.416.
[12] S.S. Hecht, Nat. Rev. Cancer 3 (2003) 733–744, https://doi.org/10.1038/nrc1190.
[13] H. Takahashi, H. Ogata, R. Nishigaki, D.H. Broide, M. Karin, Cancer Cell 17 (2010) 89–97, https://doi.org/10.1016/j.ccr.2009.12.008.
[14] S. Fischer, B. Spiegelhalder, R. Preussmann, Carcinogenesis 10 (1989) 1511–1517.
[15] H. Yuan, C. Li, R. Shan, J. Zhang, Y. Wu, Y. Chen, Fuel Process. Technol. 238 (2022), 107531, https://doi.org/10.1016/j.joei.2023.101206.
[16] H.R. Robles-Jimarez, L. Sanjuan-Navarroa, N. Jornet-Martínez, C.T. Primaz, R. Teruel-Juanes, C. Molins-Legua, A. Ribes-Greus, P. Campíns-Falcó, Sci. Total Environ. 805 (2022), 150317, https://doi.org/10.1016/j.scitotenv.2021.150317.
[17] M. Ghadermazi, S. Molaei, Catal. Surv. Asia Journal of Journal of Catalysis (2022) 1–38.
[18] M. Ghadermazi, S. Molaei, J. Porous Mater. 29 (2022) 1929–1945.
[19] M. Ghadermazi, S. Molaei, S. Khorami, J. Porous Mater. (2022), https://doi.org/10.1007/s10934-022-01398-9.
[20] M. Ghadermazi, S. Molaei, Inorg. Chem. Commun. 147 (2022), 110225, https://doi.org/10.1016/j.inoche.2022.110225.
[21] W.G. Lin, Y. Zhou, Y. Cao, S.L. Zhou, M.M. Wan, Y. Wang, J.H. Zhu, Catal. Today 212 (2013) 52–61, https://doi.org/10.1016/j.cattod.2012.07.045.
[22] Y.Y. Li, M.M. Wan, J.H. Zhu, Environ. Chem. Lett. 12 (1) (2014) 139–152, https://doi.org/10.1007/s10311-013-0451-1.
[23] G. Yong, Z. Jin, H. Tong, X. Yan, G. Li, S. Liu, Microporous Mesoporous Mater. 91 (2006) 238–243, https://doi.org/10.1016/j.micromeso.2005.12.002.
[24] A. Marcilla, M.I. Beltran, A. Gómez-Siurana, D. Berenguer, I. Martínez-Castellanos, J. Anal. Appl. Pyrolysis 119 (2016) 162–172, https://doi.org/10.1016/j.jaap.2016.02.021.
[25] A. Marcilla, M.I. Beltran, A. Gómez-Siurana, I. Martínez-Castellanos, D. Berenguer, Ind. Eng. Chem. Res. 54 (2016) 1916–1924, https://doi.org/10.1021/ie5038837.
[26] A. Marcilla, M.I. Beltrán, A. Gómez-Siurana, I. Martínez-Castellanos, D. Berenguer, Sci-Afric J. Sci. Issues. Res. Essays. 3 (2015) 571–586, https://doi.org/10.11648/j.ajche.20150301.11.
[27] A. Marcilla, A. Gómez-Siurana, D. Berenguer, I. Martínez-Castellanos, M.I. Beltrán, Toxicol Rep 2 (2015) 152–164, https://doi.org/10.1016/j.toxrep.2014.11.014.
[28] A. Marcilla, A. Gómez-Siurana, D. Berenguer, I. Martínez-Castellanos, M.I. Beltrán, Microporous Mesoporous Mater. 161 (2012) 14–24, https://doi.org/10.1016/j.micromeso.2012.05.010.
[29] P.N. Lee, S. Djurdjevic, R. Weitkunat, G. Baker, Regul. Toxicol. Pharmacol. 100 (2018) 92–104, https://doi.org/10.1016/j.yrtph.2018.10.010.
[30] C.D. Czoli, C.M. White, J.L. Reid, et al., Tobac. Control 29 (2019) 89–95, https://doi.org/10.1136/tobaccocontrol-2018-054654.
[31] K.L. Marynak, T.W. Wang, B.A. King, et al., Am. J. Prev. Med. 55 (2017) 551–554.
[32] S.H. Edwards, L.M. Rossiter, K.M. Taylor, M.R. Holman, L. Zhang, Y.S. Ding, C. H. Watson, Chem. Res. Toxicol. 30 (2) (2017) 540–551, https://doi.org/10.1021/acs.chemrestox.6b00268.

[33] J. Asensio, D. Berenguer, A. Marcilla, M.I. Beltrán, J. Anal. Appl. Pyrolysis (2023) (acepted).
[34] J. Asensio, M.I. Beltrán, N. Juárez-Serrano, D. Berenguer, A. Marcilla, Appl. Sci. 12 (19) (2022) 9426, https://doi.org/10.3390/app12199426.
[35] A. Marcilla, I. Beltrán, A. Gómez, R. Navarro, D. Berenguer, I. Martínez, Tobacco-catalyst Mixtures for Reducing the Toxic Compounds Present in Tobacco Smoke, EURO-PCT078230349, Spain, 2009.
[36] Y.Q. Yeh, H.P. Lin, C.Y. Tang, C.Y. Mou, J. Colloid Interface Sci. 362 (2011) 354–366, https://doi.org/10.1016/j.jcis.2011.07.011.
[37] T.R. Gaydhankar, V. Samuel, R.K. Jha, R. Kumar, P.N. Joshi, Mater. Res. Bull. 42 (2007) 1473–1484, https://doi.org/10.1016/j.materresbull.2006.11.006.
[38] D. Zhao, F. Zhang, B. Tu, H. Yang, C. Yu, Y. Yan, Y. Meng, J. Phys. Chem. B 109 (2005) 8723–8732, https://doi.org/10.1021/jp044632+.
[39] N.A. Fellenz, J.F. Bengoa, S.G. Marchetti, A. Gervasini, Appl. Catal. Gen. 435–436 (2012) 187–196, https://doi.org/10.1016/j.apcata.2012.06.003.
[40] P. Iliade, I. Miletto, S. Coluccia, G. Berlier, Res. Chem. Intermed. 38 (2012) 785–794, https://doi.org/10.1007/s11164-011-0417-5.
[41] M. Miura, S. Sakamoto, K. Yamaguchi, T. Ohwada, Tetrahedron Lett. 41 (2000) 3637–3641, https://doi.org/10.1016/S0040-4039(00)00431-7.
[42] J.H. Zhu, W.G. Lin, Y. Zhou, Y. Cao, S.L. Zhou, M.M. Wan, Y. Wang, Catal. Today 212 (2013) 52–61, https://doi.org/10.1016/j.cattod.2012.07.045.
[43] J.H. Zhu, S.H. Li, X.D. Sun, Y. Wang, C.L. Shi, W. Gu, W. Wang, H. Yao, Y. Wang, Chem. Eng. J. 332 (2018) 331–339, https://doi.org/10.1016/j.cej.2017.09.090.
[44] J.H. Zhu, X.D. Sun, S.H. Li, X.Y. Ming Dong, L. Wang, W.-B. Gu, W. Wang, Z.-Y. Yangand, Y. Wang, Microporous Mesoporous Mater. 243 (2017) 39–46, https://doi.org/10.1016/j.micromeso.2017.01.041.
[45] S.H. Li, X.D. Sun, Y. Wang, Z.P. Wang, W. Gu, W. Wang, H. Yao, Y. Wang, J.H. Zhu, ACS Appl. Mater. Interfaces 9 (2017) 26805–26817, https://doi.org/10.1021/acsami.7b06264.
[46] International Agency for Research on Cancer, Agents classified by the IARC monographs, Igarss 2014 1–105 (2012) 1–5, https://doi.org/10.1007/s13398-014-0173-7.2.
[47] F.J. Wiebel, Prog. Respir. Res. 42 (2015) 37–46, https://doi.org/10.1159/000369323.
[48] R. Talhout, T. Schulz, E. Florek, J. van Benthem, P. Wester, Int. J. Environ. Res. Publ. Health 8 (2011) 613–628, https://doi.org/10.3390/ijerph8020613.
[49] C.J. Smith, T.A. Perfetti, R. Garg, C. Hansch, Food Chem. Toxicol. 41 (2003) 807–817, https://doi.org/10.1016/S0278-6915(03)00021-8.